Transient Climate Change and Potential Croplands of the World in the 21st Century

Xiangming Xiao[1,3], Jerry M. Melillo[2], David W. Kicklighter[2], A. David McGuire[4], Hanqin Tian[2], Yude Pan[2], Charles J. Vorosmarty[1] and Zili Yang[3]

[1]Institute for the Study of Earth, Ocean and Space, Univ. of New Hampshire, Durham, NH 03824
[2]The Ecosystems Center, Marine Biological Laboratory, Woods Hole, MA 02543
[3]Joint Program on the Science and Policy of Global Change, MIT, Cambridge, MA 02139
[4]Institute of Arctic Biology, University of Alaska, Fairbanks, AK 99775

Abstract

A cropland distribution model, which is based on climate, soil and topography, is applied to estimate the area and spatial distribution of global potential croplands under contemporary climate and to assess the effect of transient climate changes projected by the MIT Integrated Global System Model for assessment of climate change. The area of global potential croplands is about 32.91×10^6 km^2 under contemporary climate, and increases substantially over the period of 1977–2100 and differs among the three transient climate change predictions, being about +6.7% (2.20×10^6 km^2), +11.5% (3.78×10^6 km^2), and +12.5% (4.12×10^6 km^2) in 2100, respectively. Among twelve economic regions of the world, the Former Soviet Union and the Other OECD Countries regions have the largest increases in potential croplands, while developing countries have little increases in potential croplands. Spatial distribution of potential croplands changes considerably over time, dependent upon the transient climate change predictions.

1. Introduction

Human population of the world is increasing by about 1.5% per year and is projected to double by the end of 21st Century. Increasing human population and higher demand for food may require both expansion of land used for crop production and higher yield per unit area of croplands to provide enough food supplies for people. It has been estimated that deforestation and land conversion to agriculture was about 0.3 hectare for each additional person in 1700–1980 for the whole world, and 0.2 hectare per additional person in 1950–1980 for the developing countries.[1] Using 0.2 hectare per person, Grubler[1] estimated that an increase of 10×10^6 km^2 arable lands would be needed for additional 5 billion world population in the 21st Century. Agricultural production per unit area has increased substantially over last few decades due to irrigation, fertilization, mechanization and new crops of higher yield and stronger resistance to pest and disease. Intensive agricultural production, however, is under increasing constraints of energy and resources, *e.g.*, fertilizer, water and soils.[2] Land degradation and desertification are reducing the areas of fertile lands for agriculture production.[3] At present, soil erosion has resulted in a loss of croplands at about 0.06 to 0.07×10^6 km^2 per year, and soil salinization has already affected up to 8% (0.2×10^6 km^2) of the 2.53×10^6 km^2 currently irrigated croplands.[4] Rapid expansion of urbanization has also resulted in significant losses of agricultural lands, especially in developing countries. Cultivable land per capita in China has declined approximately 20% since 1978, mostly due to rural industrialization and small-town growth.[5] Urban areas currently account for about 1% of the global land area and may increase to occupy 2% of the global land area by 2100.[6] Therefore, future trends in the area and

Corresponding author: Dr. Xiangming Xiao, Institute for the Study of Earth, Oceans and Space, University of New Hampshire, Durham, NH 03824-3525 USA. Tel: (603)862-3818, Fax: (603)862-1915, E-mail: xiangming.xiao@unh.edu
(Submitted to *Ambio*: 4/97)

spatial distribution of land used for crop production are likely to have significant impacts on sustainable agriculture and environment in the 21st Century. The question we want to address in this study is to what extent transient climate change in the 21st Century will affect the area and spatial distribution of croplands in the world.

The United Nations Food and Agriculture Organization (FAO) has developed the Agro-Ecological Zone approach to assess land suitability for croplands at local and national scales, which is based on climate, soil and crop characteristics.[7-9] The approach has been further applied at the global scale.[10, 11] By modeling the global distribution of potential croplands under contemporary climate and under doubled CO_2 equilibrium climates generated by four atmospheric general circulation models (GCMs), Cramer and Soloman[11] found that climate change significantly affects the area and spatial distribution of land that can potentially be used for crop production. However, topographical constraints on cropland distribution were not included in the above studies, and consequently the area of potential croplands is likely to be substantially overestimated.

In this study, we develop a cropland distribution model that includes climate, soil and topography constraints on the distribution of potential croplands. We apply the model to estimate the area and spatial distribution of potential croplands of the world under contemporary climate. To assess the effect of transient climate change on potential croplands, we use three transient climate change predictions over the period of 1977–2100 from the MIT Global System Model for integrated assessment of climate change.[12] The MIT framework (Fig. 1) includes the Anthropogenic Emission Prediction and Policy Analysis (EPPA) model,[13] an atmospheric chemistry model,[14] a two-dimensional climate model (MIT 2-D L-O climate model[15-19]), a terrestrial biogeochemistry model (the Terrestrial Ecosystems Model[19-22]) and natural emission models of N_2O and CH_4 from soils.[23] The EPPA model projects anthropogenic emissions of CO_2 and other greenhouse gases (*e.g.*, N_2O and CH_4) in the twelve economic regions of the world. We examine the spatial and temporal dynamics of potential croplands at the scales of the globe, economic regions and grid cells.

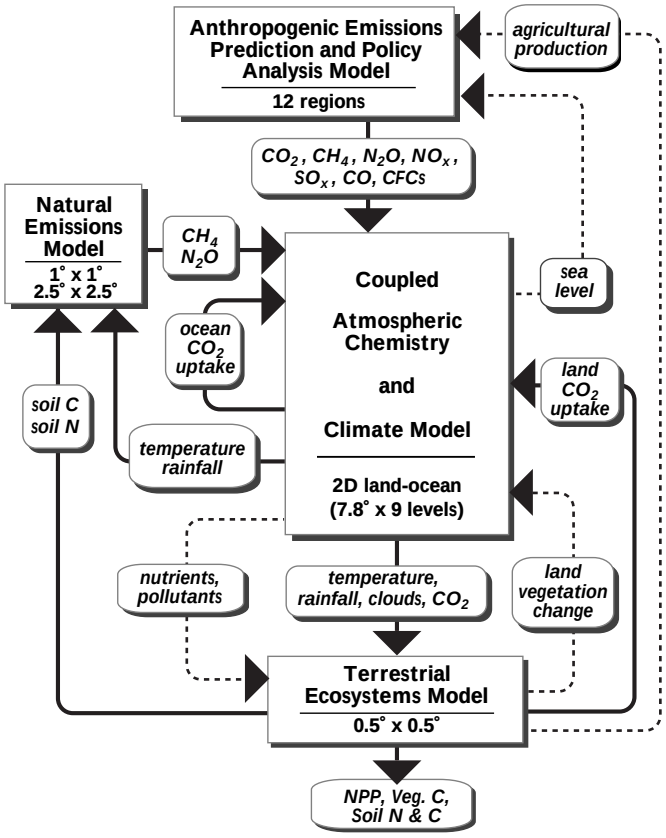

Figure 1. A schematic of the framework and components of the MIT Global System Model for integrated assessment of climate change. The linkages and feedbacks between the component models that are currently included or under development for future inclusion are shown as solid and dashed lines, respectively.

2. Cropland Distribution Model

2.1 Climate constraints

Heat and water requirements of crops determine the spatial distribution of potential croplands. In a correlation analysis between the map of croplands[24] and maps of climate variables generated from

the IIASA database of contemporary climate,[25] Cramer and Soloman[11] defined a climate envelope of potential croplands: equal or greater than 2000 growing degree days (0 ˚C base), a ratio of actual evapotranspiration over potential evapotranspiration (AET/PET) greater than 0.45; excluding those areas that have a temperature of greater than 15.5 ˚C in the coldest month and a AET/PET ratio of greater than 0.70, where potential severe soil erosion in croplands would limit crop production. The climate envelope has been used in a few global studies.[10, 11]

We also use the climate envelope of Cramer and Soloman[11] to define climate-based potential croplands in our study, although our procedures to calculate growing degree days and AET/PET ratios are slightly different from Cramer and Soloman. In our study, monthly mean temperature data are linearly interpolated to daily mean temperature, which are then used for calculating growing degree days. We use the water balance model of Vorosmarty *et al.*,[26] which has been incorporated into our Terrestrial Ecosystem Model (TEM[12, 19-22]) to estimate PET and AET. The water balance model runs at monthly time step. The input variables of the water balance model include elevation, soil texture (proportion of sand, clay and silt), monthly climate (temperature, precipitation and cloudiness) and vegetation types. Elevation is used to determine snowmelt dynamics of a grid cell (snowmelt occurs in one month if elevation is below 500 m; snowmelt occurs in two months if elevation is above 500 m). Soil texture affects the field water-holding capacity and wilting point of soils. The monthly flux PET is calculated as a function of monthly mean air temperature and solar radiation.[27] The flux of AET is equal to PET in wet months but is modeled as a function of rainfall, snowmelt recharge and a change of soil moisture in dry months.[26] The ratio of AET/PET for each of twelve months is calculated. For moist tropical regions where temperature in the coldest month is greater than 15.5 ˚C, we assume that a grid cell will not be suitable for croplands if there are more than eight months in a year that have a AET/PET ratio greater than 0.70.

2.2 Topographical constraints

Cropland distribution is also constrained by topographical features such as slope and aspect, because cropland is vulnerable to soil erosion and low stability of slope in mountainous regions. In land use planning at the fine spatial scale, slope and aspect are widely used to determine whether land is suitable for crop cultivation. However, at large spatial scales such as 0.5˚ latitude × 0.5˚ longitude, slope generally has very small values, because of the large denominator (*e.g.*, 55 km at equator) in the calculation of slope, and therefore is no longer as meaningful as it is at fine spatial scales. Instead, we use elevation data directly to define mountains. Mountain systems account for roughly 20% of the global land area.[28] Mountain regions are characterized by multiple land uses, *e.g.*, forestry, minerals mining, hydropower plant and tourism.

For defining mountains from elevation data, we designed a pattern search algorithm within a window that has 3 × 3 grid cells. We calculate elevation differences between the center grid cell and each of its eight neighboring grid cells. We first recognize or stratify three topographical features of the world: plains with low elevation (approximately lower than 500 m in elevation); low mountains and low plateau (approximately lower than 1000 m in elevation); high mountains and high plateau (*e.g.*, Rocky mountains in north America, Andes in south America, Himalayas mountains, Qinghai-Tibet plateau in China). Then, we apply the following criteria to decide whether the center grid cell is mountain: (1) elevation difference is greater than 400 m, when elevation of the center grid cell is less than 500 m; (2) elevation difference is greater than 600 m, when elevation of the center grid cell is within 500–1000 m; and (3) elevation difference is greater than 1200 m, when elevation of the center grid cell is more than 1000 m. If any of the eight elevation differences within a 3 × 3 window meets one of the criteria, then the center grid cell is assigned to be mountain. If a grid cell is assigned to be mountain, it will not be used for cropland, even if it meets climate constraints for croplands. We used this 3 × 3 window pattern search for all the grid cells in our global elevation database,[29]

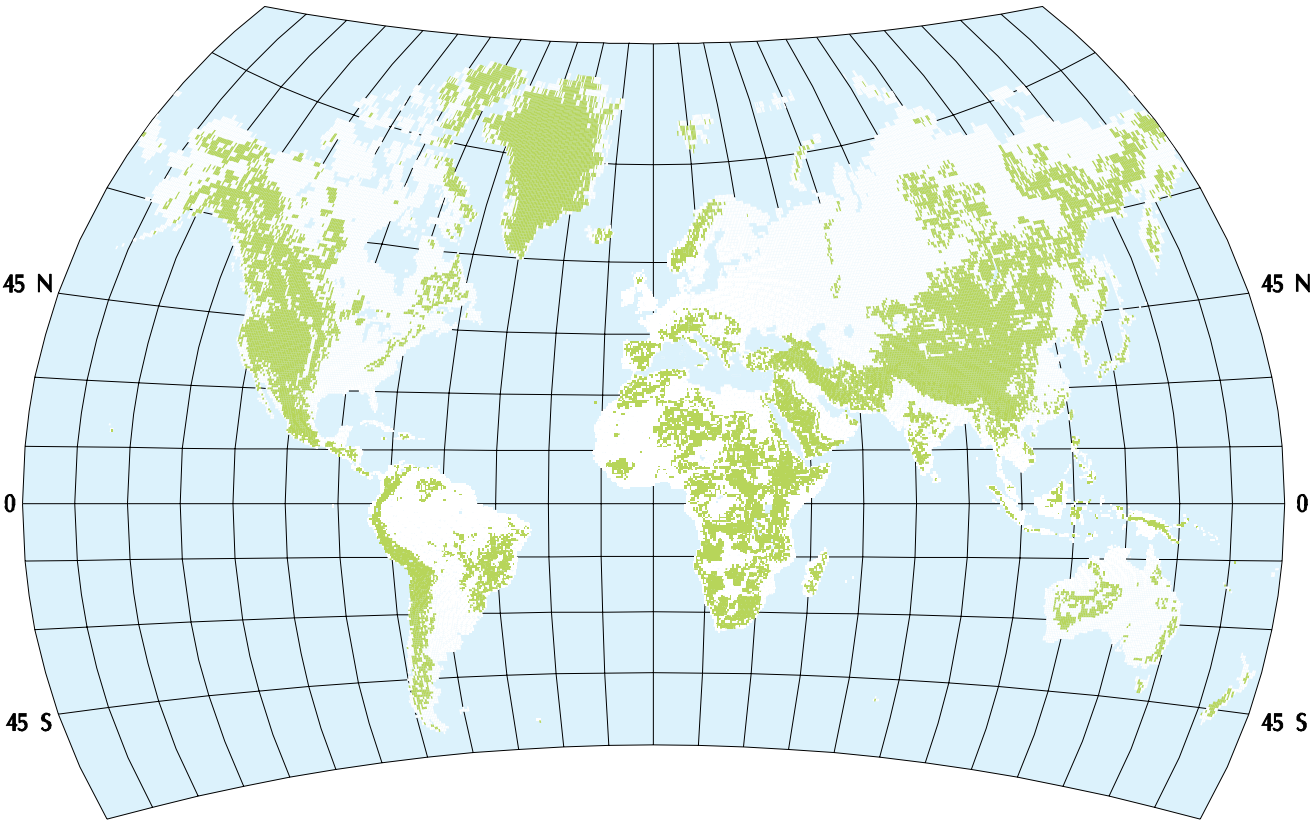

Figure 2. Spatial distribution of mountains in the world. Note that Greenland is mostly covered with ice.

which has a resolution of 0.5˚ longitude × 0.5˚ latitude grid. The resulting global map of mountain (Fig. 2) clearly shows large mountain ranges, *e.g.*, Rocky, Andes and Qinghai-Tibet plateau. In a visual qualitative comparison, the geographical distribution of mountains in our global map of mountains mimics well with a shaded relief image of global topography,[30] which was generated from an elevation data set (NOAA's ETOPO5) with a spatial resolution of 5´ latitude by 5´ longitude.

2.3 Data for global extrapolation

The spatial data sets used for a global extrapolation of the cropland distribution model are organized at a resolution of 0.5˚ longitude × 0.5˚ latitude grid, including elevation,[29] soil texture,[31] vegetation types[21] and long-term average contemporary climate from the Cramer and Leemans CLIMATE database (Wolfgang Cramer, person communication), which is a major update of the IIASA Climate database.[25] Of the 62,483 land grid cells in these spatial data sets, there are 3,059 ice grid cells and 1,525 wetland grid cells (*e.g.*, mangrove, swamp, salt marsh and flood plains). Thus, the global land area used in this study is 133.56×10^6 km^2, *i.e.*, 130.31×10^6 km^2 upland and 3.25×10^6 km^2 wetlands. In calculating potential croplands, we exclude those grid cells that are wetland in the vegetation data set.[21] We run the cropland distribution model using the above global data sets to estimate spatial distribution of potential cropland under the contemporary climate.

2.4 Transient climate change scenarios

To assess the sensitivity of potential croplands to future climate change, we used transient climate change predictions over the period of 1977–2100 from a sensitivity study of the MIT Global System Model.[12] In the sensitivity study, the standard parameters and assumptions in the EPPA model and the atmospheric chemistry/climate model were first used to generate the 'Reference' scenario of changes in anthropogenic emissions of greenhouse gases and climate. Anthropogenic

emissions of CO_2 projected by the EPPA model in the 'Reference' scenario are similar to the CO_2 emissions of the IS92a scenario of IPCC.[32] Then, the EPPA model projected higher and lower emissions of CO_2 and other greenhouse gases by changing the labor productivity growth, the non-price-induced change in energy efficiency (AEEI rate) and the cost of non-carbon backstop technology (*e.g.*, nuclear and solar energy). The emissions of CO_2 and other greenhouse gases were used to drive the combined atmospheric chemistry/MIT 2-D L-O climate model. In the MIT 2-D L-O climate model, parameters for ocean heat diffusion efficiency, aerosol optical depth and model sensitivity to doubled CO_2 were changed to generate different climate change predictions for a given set of emissions of CO_2 and other greenhouse gases. Seven transient climate change predictions over the period of 1977–2100 have been generated in the sensitivity study.[12] Here, we used three of the seven transient climate change predictions: (1) the 'Reference' scenario; (2) the 'HHL' scenario that has higher CO_2 emissions from the EPPA model and larger changes in temperature from the climate model, which uses parameters of higher temperature sensitivity to doubled CO_2 and lower heat diffusion coefficient into the deep ocean; and (3) the 'LLH' scenario that has lower CO_2 emissions from the EPPA model and smaller changes in temperature from the climate model, which uses parameters of lower temperature sensitivity to doubled CO_2 and higher heat diffusion coefficient into the deep ocean. Globally, atmospheric CO_2 concentration and climate vary significantly among the three transient climate change predictions over the period of 1977–2100 (Fig. 3). Atmospheric CO_2 concentration in 2100 is about 745 ppmv in the 'Reference', 936 ppmv in the 'HHL' and 592 ppmv in the 'LLH' scenarios. Global annual mean temperature between 1977 and 2100 increases about 2.6 ˚C for the 'Reference', 3.3 ˚C for the 'HHL' and 1.4 ˚C for the 'LLH' scenarios. Global daily precipitation increases slightly over time for the three scenarios. Global mean annual cloudiness decreases in the 'Reference' and the 'LLH' scenarios but increases in the 'HHL' scenario.

The MIT 2-D L-O climate model simulates the zonally averaged climate separately over land and ocean as a function of latitude and height. It has 23 latitudinal bands, corresponding to a resolution of 7.826˚, and nine vertical layers. The climate outputs in the 23 latitudinal bands from the MIT 2-D L-O climate model were first linearly interpolated to 0.5˚ resolution, and the interpolated values were then applied to all the grid cells within a 0.5˚ latitudinal band. In generating "future

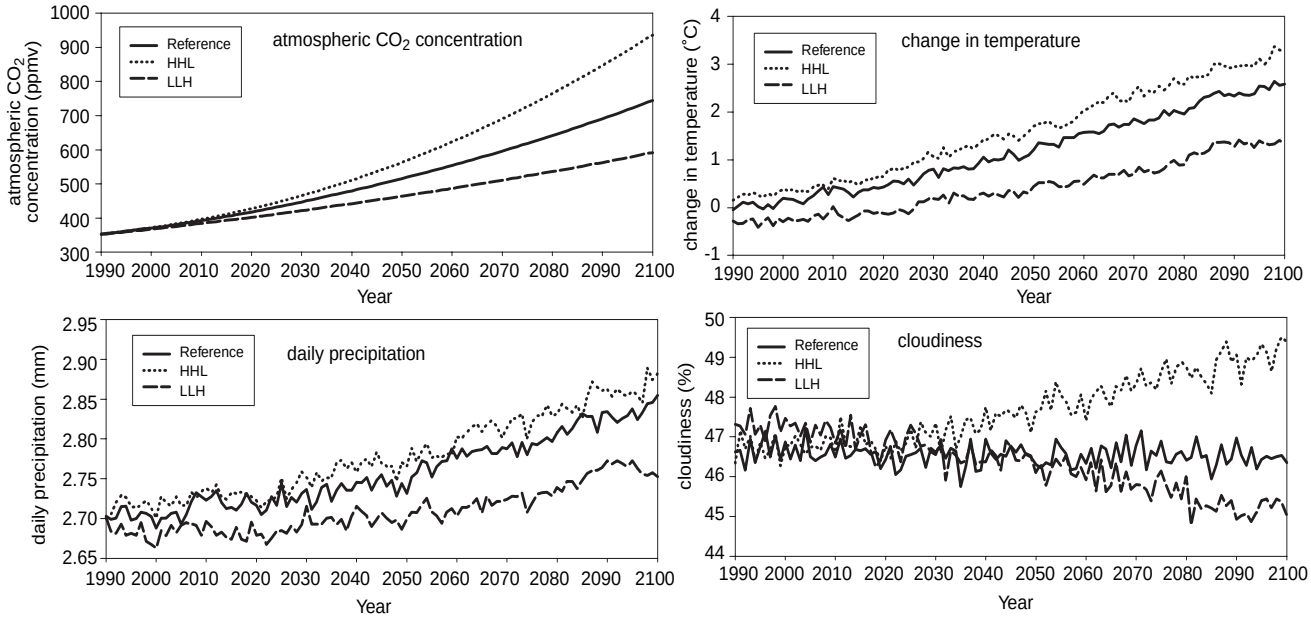

Figure 3. Projected changes in global annual mean atmospheric CO_2 concentration (ppmv), global annual mean temperature (˚C), global mean daily precipitation (mm) and global annual mean cloudiness (%) over the period of 1977–2100 for the Reference, HHL and LLH scenarios by the MIT 2-D L-O climate model (see reference 12 for details).

climate" we calculated absolute differences in monthly mean temperature and ratios in monthly precipitation and monthly mean cloudiness, using the simulated climate data in 1977 from the MIT 2-D L-O climate model as the control values. Then, we added the absolute differences in monthly mean temperature over the period of 1978–2100 to the contemporary monthly mean temperature data, and multiplied the ratios in monthly precipitation and monthly mean cloudiness over the period of 1978–2100 by the contemporary monthly precipitation and monthly mean cloudiness data, respectively.

3. Results and Discussion

3.1 Potential croplands under contemporary climate

The cropland distribution model estimates that the area of global potential croplands under contemporary climate is about 32.91×10^6 km^2, approximately 25.3% of the global land area (130.31×10^6 km^2). This estimate is significantly lower than the global estimate of 41.53×10^6 km^2 potential croplands by Cramer and Soloman,[11] who modeled the potential cropland distribution using contemporary climate data.[25] This difference is primarily attributed to the fact that topographical constraint is taken into account in our cropland distribution model, and indicates that topography is important in determining potential croplands. Our estimate is about 36.4% higher than the estimate of croplands (about 24.12×10^6 km^2) of Olson *et al.*[24] and is close to the estimate of croplands (about 32.05×10^6 km^2) of Matthews.[33] Olson *et al.* and Matthews estimated global croplands by compiling map data from various data sources and available maps. For global distribution of croplands, Olson *et al.* uses a $0.5^\circ \times 0.5^\circ$ resolution grid and Matthews uses a $1.0^\circ \times 1.0^\circ$ resolution grid. Note that the above four estimates of potential cropland area are obtained with an assumption that a grid cell is 100% used for croplands if it is suitable for cultivation. In reality, the percent area used for croplands within a grid cell (*i.e.*, cultivation density) varies among grid cells and is most likely much lower than 100%, because of human settlement (*e.g.*, urban, villages), infrastructure and other types of land use. According to the FAO country statistics of cultivation,[34] approximately 15×10^6 km^2 area was actually growing crops in 1984.

Potential cropland area varies substantially among the twelve economic regions of the world used in the EPPA model (Fig. 4). The ratio of potential cropland area over total land area for each of the economic regions indicates the potential of land for cultivation. The ratio varies from 11.1% in the Energy Exporting Countries (EEX) economic region to 77.7% in the Eastern European Countries (EET) economic region (Fig. 4). The EEX and the Rest of the World (ROW) economic regions have large areas of desert and semi-arid land, where there is not enough precipitation to support rain-fed agriculture. The Former Soviet Union (FSU) and the Other OECD Countries (OOE) economic regions have large areas of land in high latitudes where the temperature is too low for crops to grow. China has the largest population in the world but a low ratio of potential cropland area over total land area, because China has large areas of mountains (Fig. 2), dry land (*e.g.*, Mongolia plateau, Gobi desert in northwestern China) and the cold Qinghai-Tibet plateau.

Actual cropland areas among the twelve economic regions in 1980, which are derived from the FAO country statistics data of crop cultivation and production,[35] vary considerably (Fig. 4), partly because of the differences in population and agricultural practices. The ratio of actual cropland area over potential cropland area indicates the realized potential of land used for cultivation (Fig. 4). The ratio ranges from 25.0% in Brazil to 109.7% in India. Only five economic regions (Brazil, Japan, OOE, FSU, and USA) have a ratio lower than 50%. The low ratio in Brazil indicates that Brazil has a large amount of potential croplands for future use. The highest ratio in India indicates that people in India have already practiced crop cultivation in a fair amount of mountainous regions and other marginal lands. However, crop cultivation in mountains is generally very vulnerable to severe soil erosion and low slope stability in mountains, especially on long-term temporal scales.

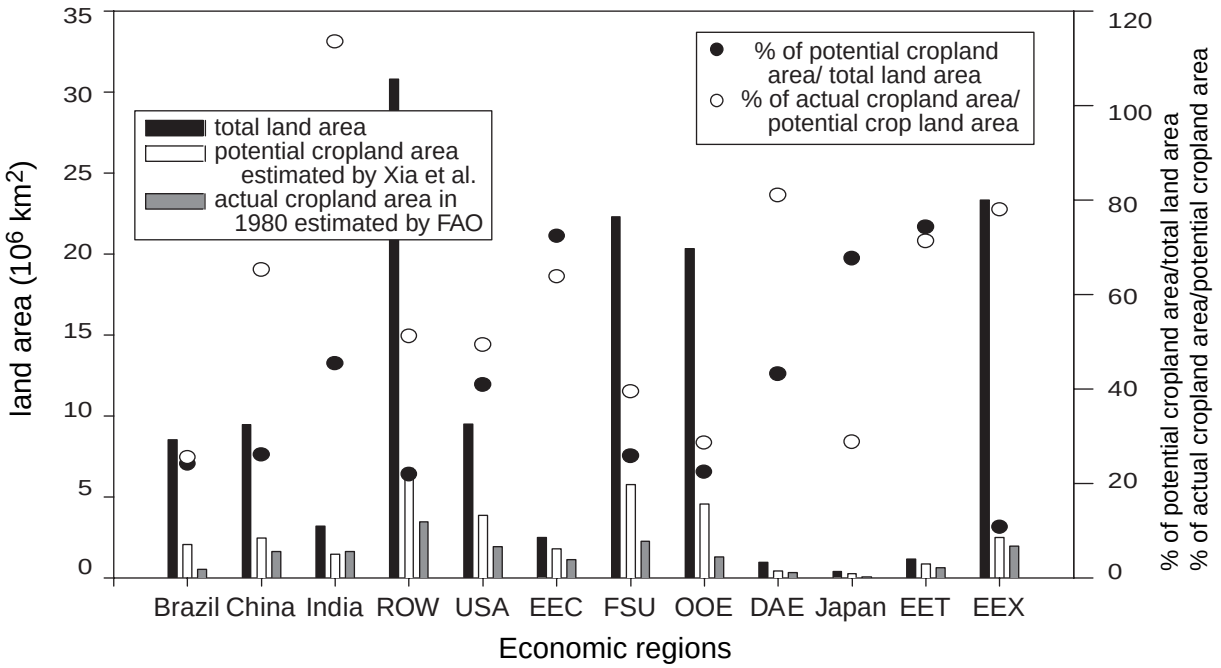

Figure 4. Total land area, potential cropland area under contemporary climate, and actual cropland area in 1980 in the twelve economic regions of the world. The regions are defined in the Anthropogenic Emission Prediction and Policy Analysis model (EPPA): Dynamics Asian Economics (DAE), European Economic Community (EEC), Eastern European Countries (EET), Energy Exporting Countries (EEX), Former Soviet Union (FSU), the Other OECD Countries (OOE), the Rest of the World (ROW), United States of America (USA). Data of actual cropland area in 1980 are aggregated from the FAO country statistics data of agricultural production (provided by Dr. G. Esser). Note that for Brazil, the ratio of potential cropland area over total land area is overlapped with the ratio of actual cropland area over potential cropland area.

As shown in Fig. 5, our cropland distribution model represents reasonably well the spatial distribution of global croplands as described in the map of croplands of Olson *et al.*[24] The agreement between Olson *et al.* and our model occurs in 6266 grid cells, about 14.35×10^6 km^2, which accounts for 59.5% of the global cropland area estimated by Olson *et al.* Olson *et al.* includes irrigated croplands, thus, a fair amount of croplands described by Olson *et al.* is located in semi-arid and arid regions. We have not included global river networks in this study and thus we can not project those croplands that are completely dependent upon irrigation from river water, *e.g.*, the Nile River (Fig. 5). A large area of croplands in the western United States is also dependent on irrigation water from aquifers.

The geographical distribution of potential croplands (Fig. 5) is closely correlated with the geographical distribution of human population (Fig. 6). Potential croplands occur mostly in those areas that have population densities of five or more people per square kilometer. Among the twelve economic regions, India and China have the highest population densities, indicating the highest pressure on potential croplands to be converted for crop cultivation. The cropland model estimates that large portions of moist tropical forests in Brazil, tropical Asian countries (*e.g.*, Philippine, Indonesia and Malaysia) and Africa are not good for croplands due to the potential of severe soil erosion in croplands (Fig. 5). In the map of Olson *et al.*,[24] there are only small areas of croplands in the moist tropical forests in Brazil but fair amounts of croplands in the tropical Asian countries where irrigated rice paddy dominates (Fig. 5). The difference between Brazil and the tropical Asian countries may be attributed primarily to much higher population pressure for crop production in the tropical Asian countries from higher population density (more than 50 people per km^2; see Fig. 6) and secondarily to monsoon climate in Asia. Our cropland distribution model estimates that a large portion of eastern Amazon is suitable for croplands (Fig. 5), where extensive deforestation has been observed during the 1980s, with a fair portion of forest conversion to croplands and pasture. Skole

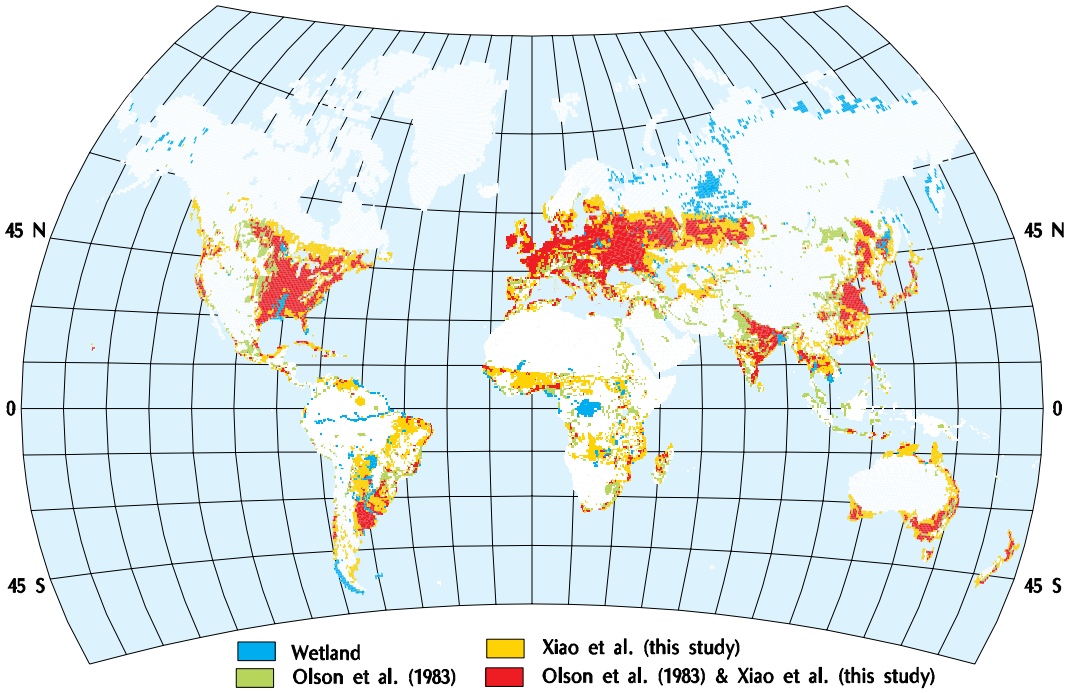

Figure 5. The comparison between the map of croplands of Olson *et al*.[24] and the map of global potential croplands under contemporary climate estimated by our cropland distribution model. Both cultivation and secondary vegetation areas are included in the map of Olson *et al*. Both maps have a spatial resolution of 0.5˚ latitude × 0.5˚ longitude.

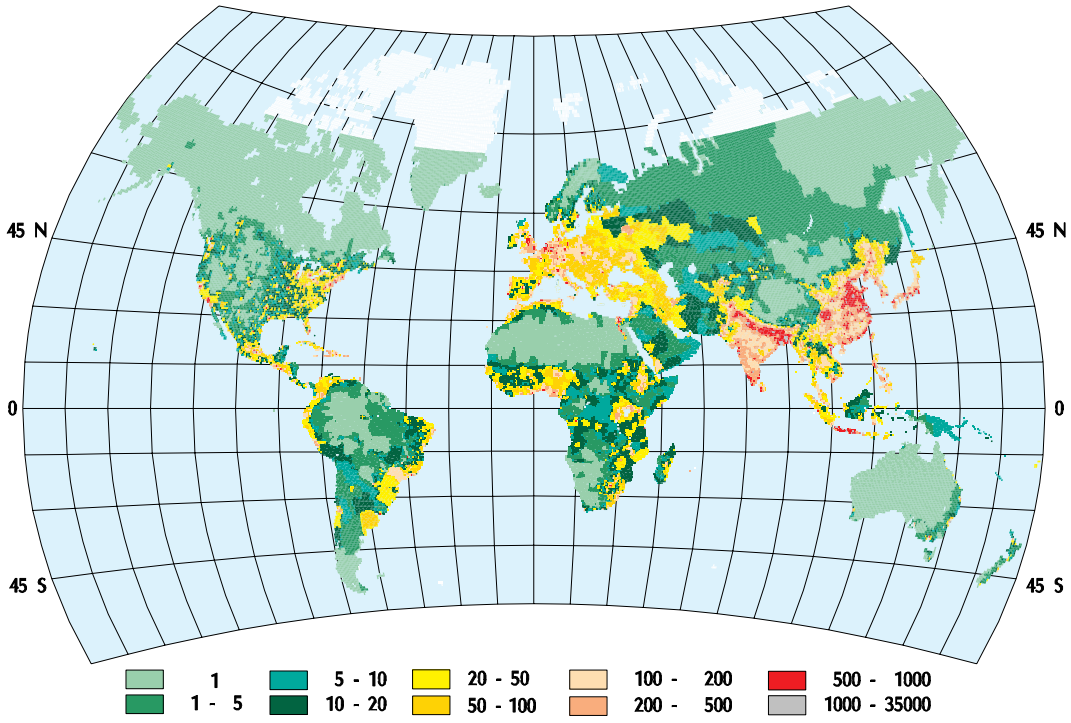

Figure 6. Geographical distribution of population density (number of people per km^2) of the world in 1994 at 0.5˚ latitude × 0.5˚ resolution. It is aggregated from the *Gridded Population of the World* at 5′ × 5′ (latitude × longitude) resolution, which was released in 1995 by the Consortium for International Earth Science Information Network (CIESIN) and the U.S. National Center for Geographical Information and Analysis (NCGIA)[47] (see also the web site at http://www.ciesin.org). The unsmoothed CIESIN and NCGIA population data covers areas from 57˚S to 72˚N.

and Tucker[36] estimated that deforested area in Amazon is 78,000 km^2 in 1978 but 230,000 km^2 in 1988, using high resolution LANDSAT imagery. Deforestation in tropical regions is closely driven by increases in human population and other social-economic factors across local, regional, national and international levels.[37-39] In this study, our cropland distribution model has not included the spatial distribution of human population. The comparison in geographical distributions between potential croplands and human population indicates that further studies are needed to quantify the relationship between cropland distribution and spatial distribution of human population. Thus, future work needs to incorporate the spatial-temporal dynamics of human population into our cropland distribution model for estimating distributions of actual croplands. Further studies are also needed to investigate the relationship between croplands and monsoon climate, especially in the above tropical Asian countries.

3.2 The effects of transient climate change on potential croplands

The area of global potential croplands increases under the three transient climate change predictions over the period of 1977–2100 (Fig. 7). The large interannual variation in the area of global potential croplands shows the effect of interannual variation of climate (Fig. 7). In 2100, the area of global potential croplands increases about 11.5% (3.78×10^6 km^2) for the 'Reference', 12.5% (4.12×10^6 km^2) for the 'HHL', and 6.7% (2.20×10^6 km^2) for the 'LLH' transient climate change predictions. The projected area of global potential croplands is slightly higher under the 'HHL' climate change prediction than under the 'Reference' climate change prediction, although temperature changes are much larger in the 'HHL' scenario than in the 'Reference' scenario (Fig. 3). In a modeling study using doubled CO_2 equilibrium climates from four GCMs (OSU, GISS, GFDL and UKMO), Cramer and Soloman[11] estimated that the area of global potential croplands increases from about 18% under the OSU climate to about 38% under the UKMO climate. The difference in areal changes of global potential croplands between our study and Cramer and Soloman[11] is partly due to the fact that our model has taken into account topographical constraints on cropland distribution.

The increase in global potential croplands is mostly attributable to increases in potential croplands of the Former Soviet Union and the Other OECD Countries economic regions (Fig. 8). The other ten economic regions have little change in the area of potential croplands. China may even have a small decrease in the area of potential croplands by the end of 21st Century. The relative

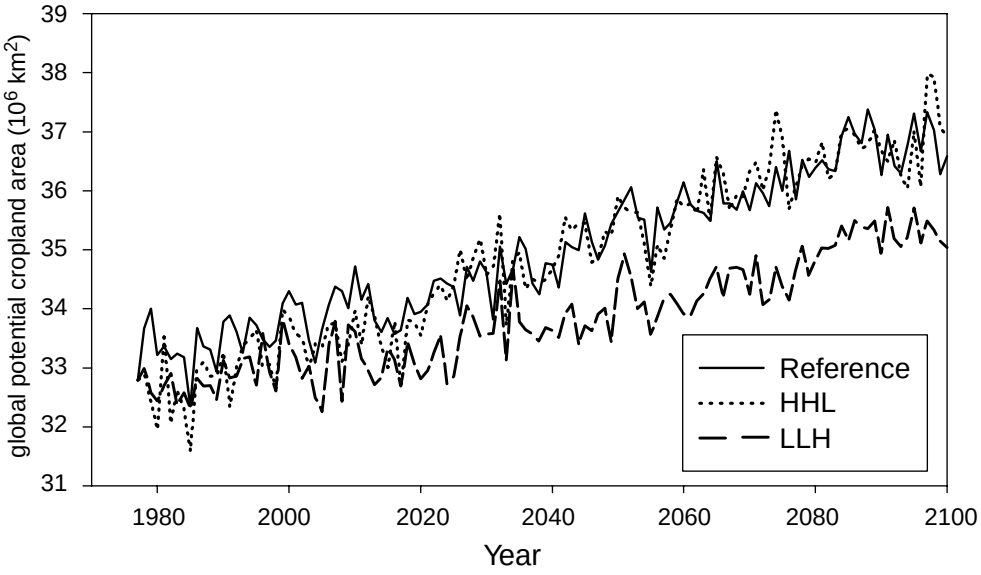

Figure 7. Temporal changes in the area of global potential croplands over the period of 1977–2100 under the three transient climate change predictions projected by the MIT 2-D L-O climate model.

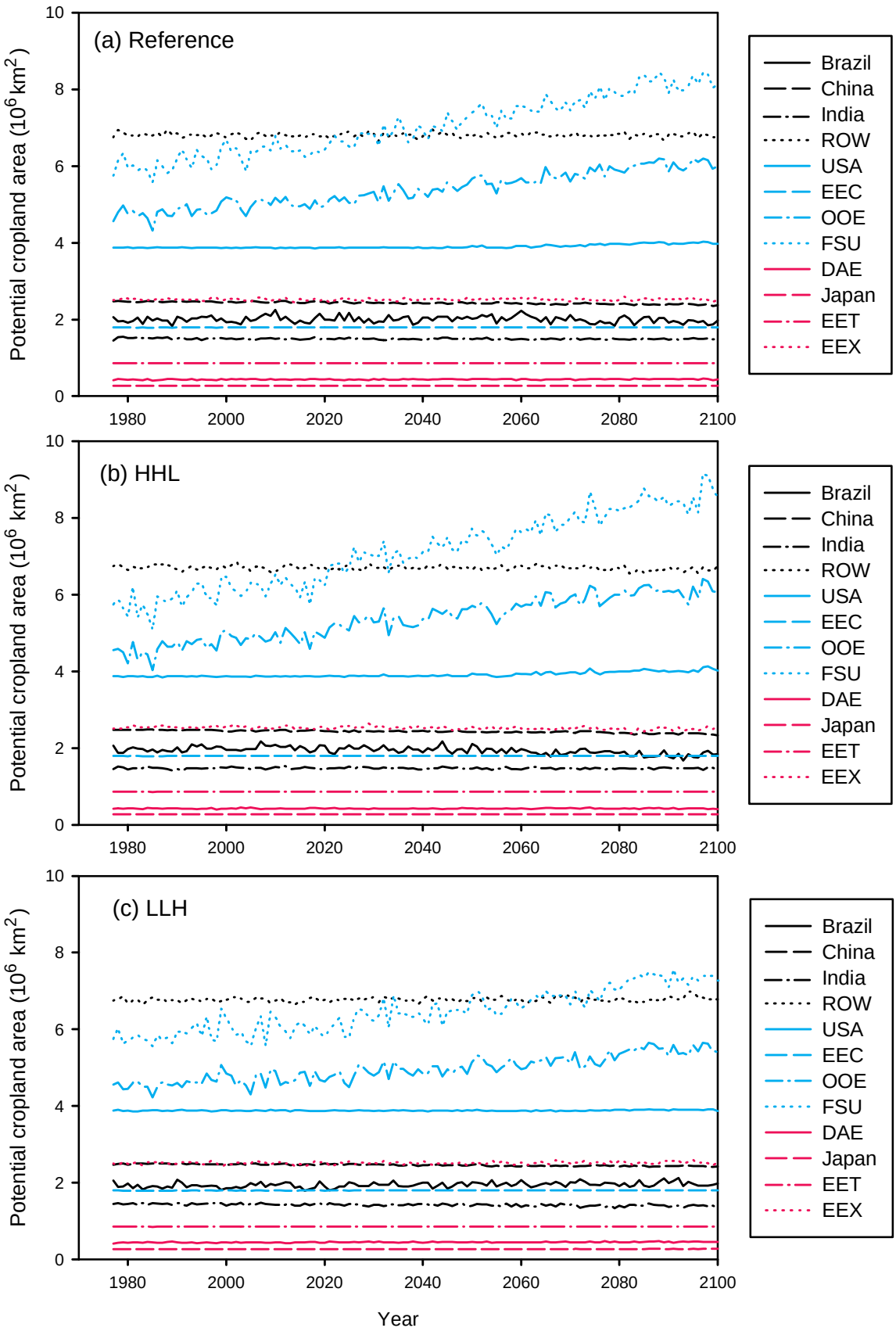

Figure 8. Temporal changes in the areas of potential croplands in the twelve economic regions over the period of 1977–2100 under the three transient climate change predictions. The acronyms for the economic regions are the same as given in Figure 4.

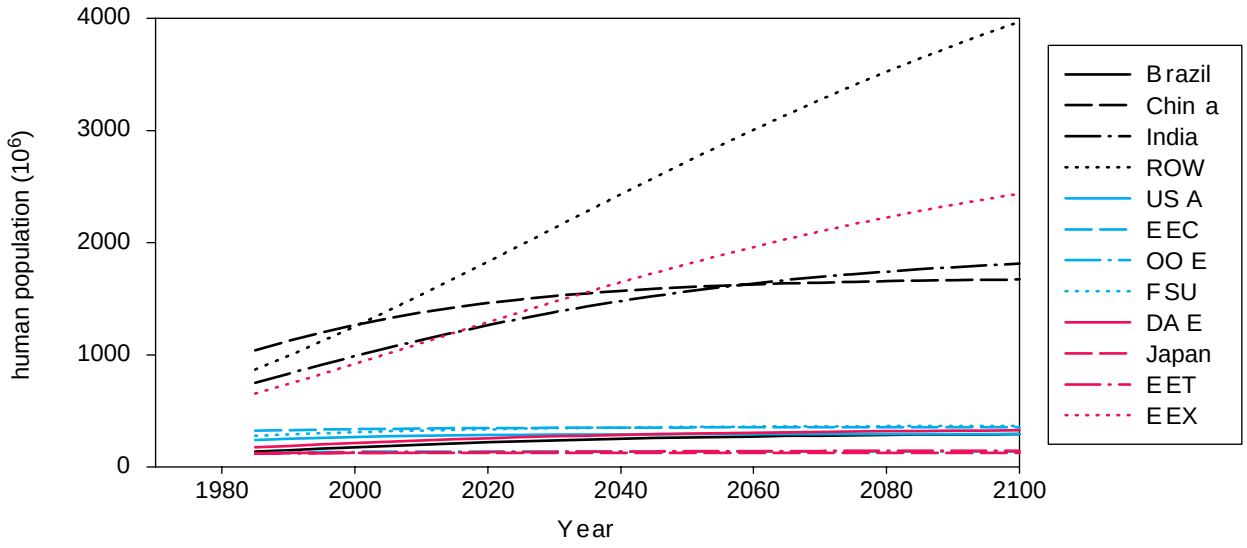

Figure 9. Temporal changes of human population in the twelve economic regions over the period of 1985–2100. These projections by the Anthropogenic Emission Prediction and Policy Analysis model (EPPA) are based on the estimates of United Nations (see reference [48]). The acronyms for the economic regions are the same as in Figure 4.

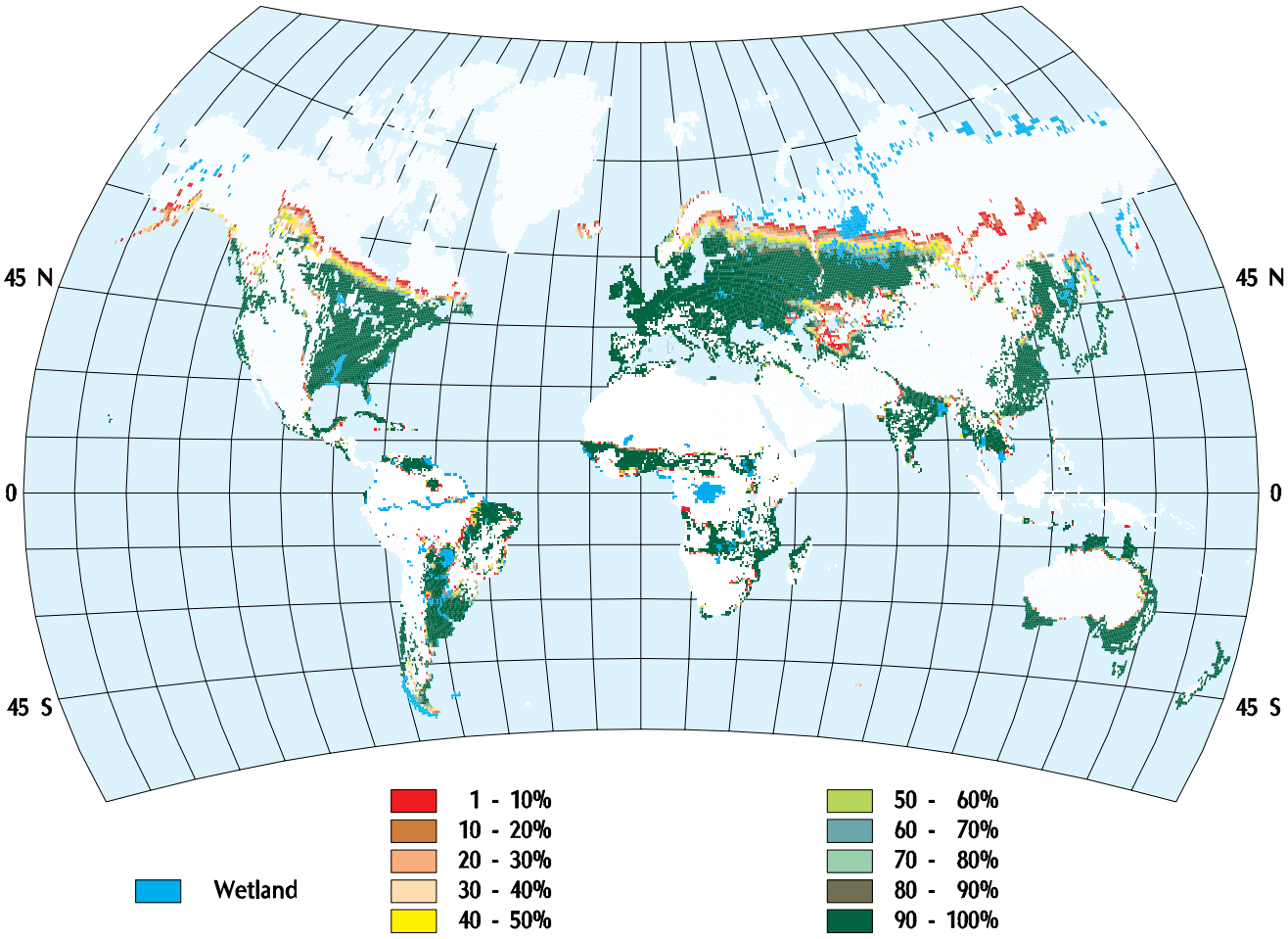

Figure 10. Changes in the spatial distribution of global potential croplands over the period of 1977–2100 under the Reference transient climate change prediction. Percentages in the color legend represent the number of years a grid cell is suitable for cropland over the 124-year simulation in the study.

contributions among the 12 economic regions to the increase of global potential croplands are similar for these three climate change predictions (Fig. 8). Human population is likely to increase substantially in developing countries, *e.g.*, China, India, and the ROW economic regions, while developed countries (*e.g.*, USA, EEC, OOE and FSU economic regions) have a small increase in population (Fig. 9). Human populations in the Dynamic Asian Economics, the Energy Exporting Countries and Brazil economic regions (Fig. 9) also increase faster than the increase in potential croplands (Fig. 8). For developing countries, the opposite trends in population and potential cropland area indicate an increasing pressure to raise agricultural production per unit area. These developing countries, however, are under the largest constraints in energy and resources, which are essential for intensive agricultural production. Future climate change and an increase of atmospheric CO_2 concentration are also likely to affect crop production significantly.[40-42] In a recent study that uses comparable crop yield models with doubled CO_2 equilibrium climate changes from three GCMs (GISS, GFDL, UKMO) to assess the potential impacts of climate change on world food supply, the results suggest that doubling of atmospheric CO_2 concentration will lead to a small decrease in global crop production.[42] Climate change increases cereal production per hectare in the developed countries but reduces cereal production per hectare in developing countries.[42] One important implication from the comparison among population dynamics, potential cropland area dynamics and crop production per hectare is that international trade in agricultural products will have to be substantially increased between developed countries and developing countries, in order to avoid food shortage in some countries in the 21st Century.

Geographically, potential croplands expand gradually into high latitudes of the northern hemisphere over the period of 1977–2100 (Figs. 10, 11, 12). The northward expansion of potential croplands is the largest in the 'HHL' but the lowest in the 'LLH' climate change predictions. Russia and Canada have the largest increases in potential cropland area, which is mostly attributed to temperature increases in high latitudes. The MIT 2-D L-O climate projected a larger temperature increase in high latitudes than in low latitudes,[12] which is consistent with the results of 3-D GCMs.[43] In high latitudes where tundra and boreal forests dominate, large portions of soils are spodosols and histosols. Physical properties (*e.g.*, water-saturation in histosols) and chemical properties (*e.g.*, pH, cation exchange capacity) of these soils may also constrain distribution of croplands, therefore, large amounts of additional resources and inputs (*e.g.*, drainage, lime application) are needed to make the soils suitable for crop cultivation. Kazakhstan, Uzbekistan and Turkmenistan in the Former Soviet Union economic region have large increases in potential cropland area. In the southern hemisphere, Brazil and Australia have small increases in potential cropland area. Cramer and Soloman[11] also projected a northward expansion of potential croplands into high latitudes under the doubled CO_2 equilibrium climates projected by the four GCMs (OSU, GISS, GFDL and UKMO). The MIT 2-D L-O climate model projects less spatial variation in climate than the 3-D GCMs because it has no variation among the grid cells along longitudes. A number of 3-D coupled atmospheric-ocean GCMs have simulated transient climate changes over time,[44] thus it would be useful to use them to drive the cropland distribution model to examine the effects of longitude and latitude variations in climate change on potential croplands. If driven by transient climate change predictions of 3-D GCMs, our cropland distribution model may give larger spatial and temporal variations in global potential croplands. However, one limitation of these coupled atmospheric-ocean GCMs experiments[44] to our study here is that they provide only one transient scenario of CO_2 change over time, and most of them use 1% CO_2 increase per year over time.

The potential expansion of croplands into high latitudes in the northern hemisphere in the 21st Century may have a significant impact on the global carbon budget. Total carbon storage (vegetation carbon plus reactive soil organic carbon) under contemporary climate at 315 ppmv CO_2 has a bimodal distribution along 0.5˚ latitudinal bands (Fig. 13). Of 1658.6 PgC (10^{15} g C) total carbon storage of the terrestrial biosphere,[19] 423.6 Pg (25.5%) is stored within the tropical latitudes (10 ˚S to

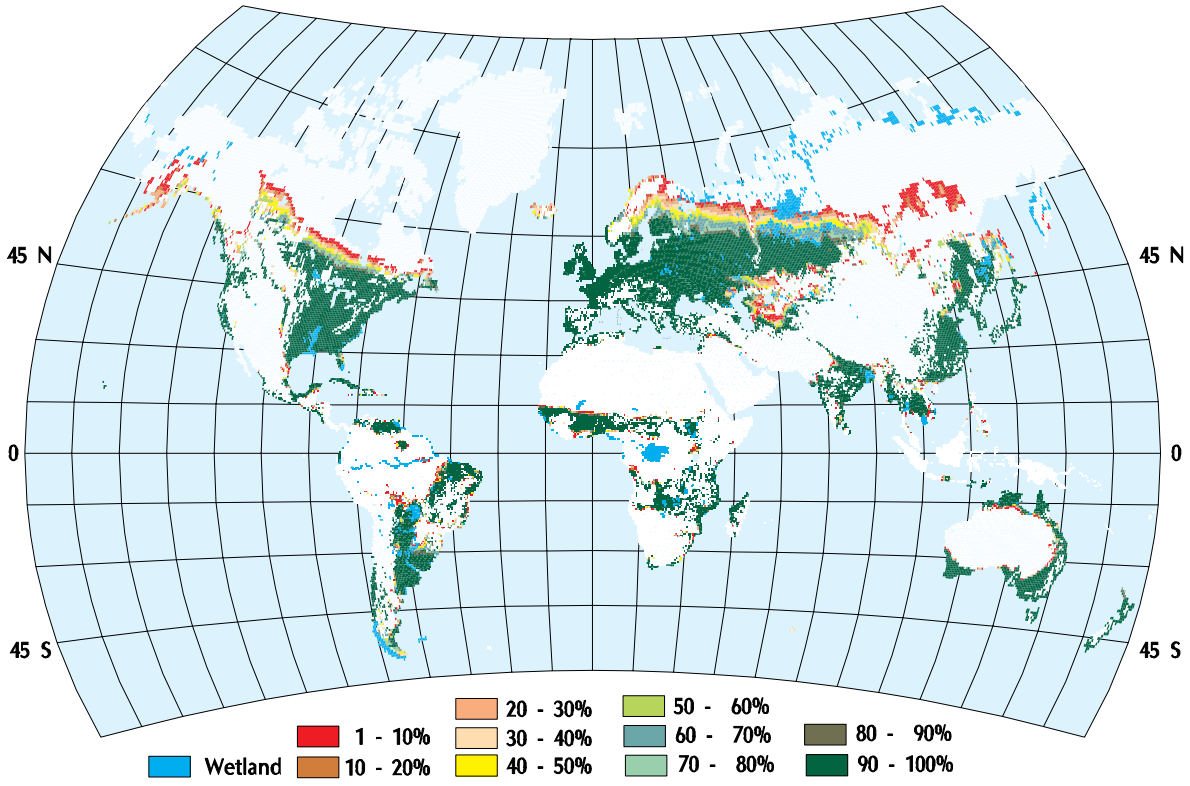

Figure 11. Changes in the spatial distribution of global potential croplands over the period of 1977–2100 under the HHL transient climate change prediction. Percentages in the color legend represent the number of years a grid cell is suitable for cropland over the 124-year simulation in the study.

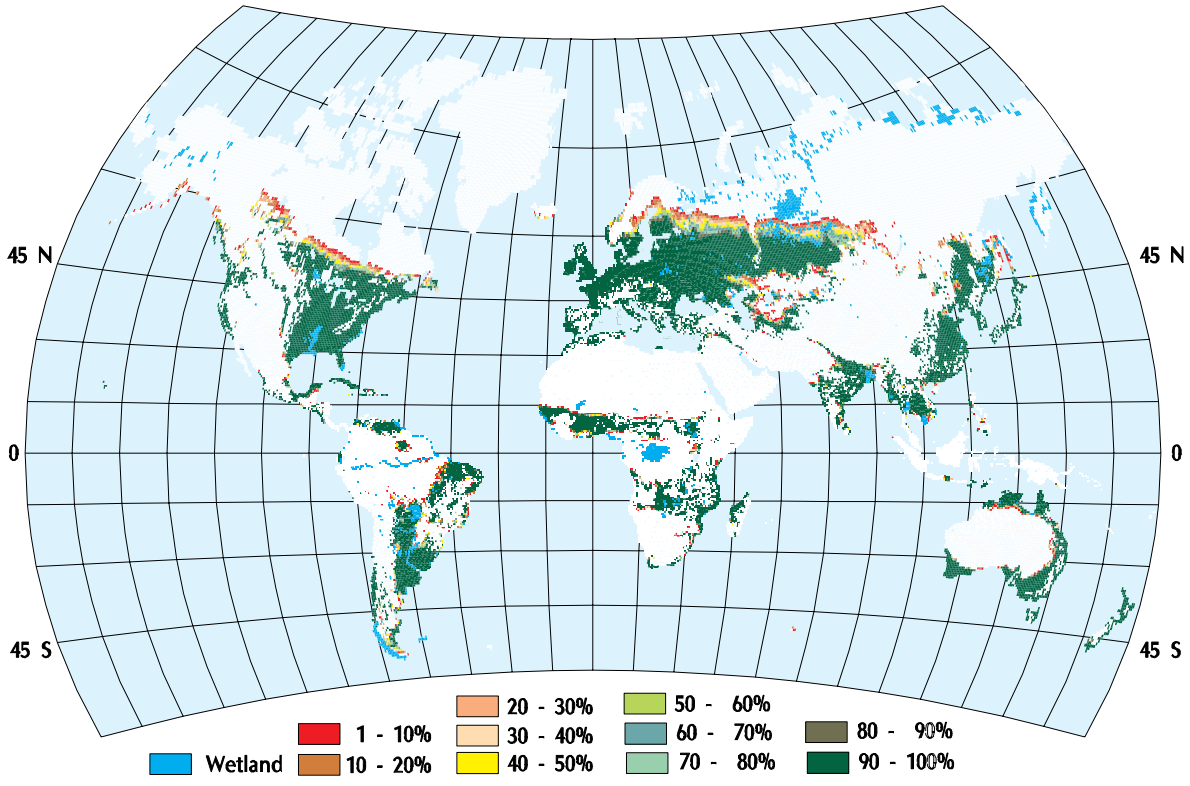

Figure 12. Changes in the spatial distribution of global potential croplands over the period of 1977–2100 under the LLH transient climate change prediction. Percentages in the color legend represent the number of years a grid cell is suitable for cropland over the 124-year simulation in the study.

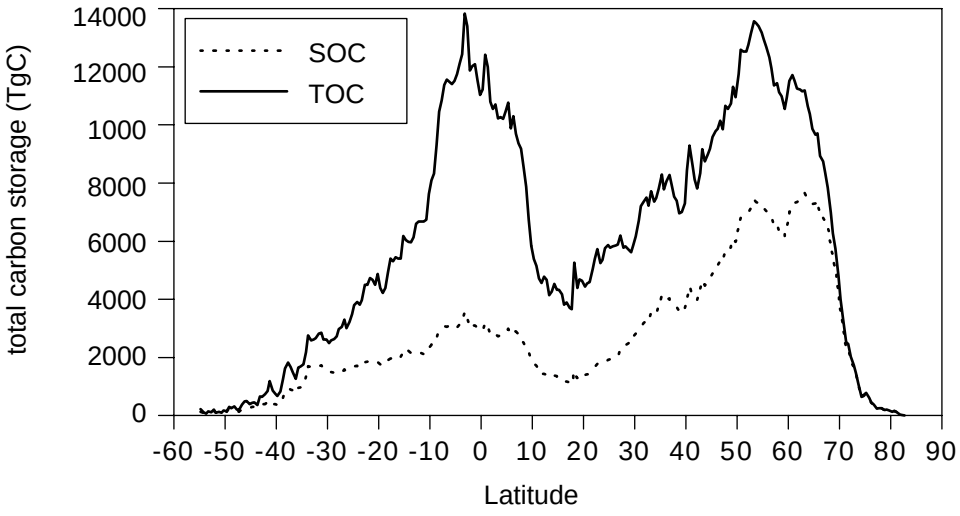

Figure 13. Latitudinal distribution of total carbon storage (TOC) and reactive soil organic carbon (SOC) for contemporary climate with 315 ppmv CO_2 along 0.5˚ resolution latitudinal bands, as estimated by the Terrestrial Ecosystem Model (see reference 19). Total carbon storage estimated by TEM is the sum of vegetation carbon and reactive soil organic carbon. Estimates of reactive soil organic carbon in a grid cell exclude inert soil organic carbon. Vegetation carbon is the difference between total carbon storage (TOC) and reactive soil organic carbon (SOC).

10 ˚N) where tropical forests dominate, and 420.8 PgC (25.4%) is stored within the 45 ˚N to 65 ˚N latitude band, where boreal forests and tundra dominate. In tropical forest ecosystems, vegetation carbon is substantially higher than reactive soil organic carbon, while a large portion of carbon in boreal forests and tundra is stored in soils. In calculating the effects of land cover and land use changes on the historical and present global carbon budget,[45, 46] tropical deforestation plays a dominant role in CO_2 emissions from land use and land cover changes. Conversion of boreal forests and tundra into croplands may also result in a large loss of carbon in vegetation and soils, and will affect carbon flux and storage in the terrestrial biosphere. Our study implies that the effort to stabilize atmospheric CO_2 concentration in the next centuries may also need to take into consideration the constraints of land use and land cover changes at the mid- to high- latitudes of the northern hemisphere.

4. Conclusion

The cropland distribution model, which is currently based on climate, soil and topography, represents reasonably well the spatial distribution of croplands in the world under contemporary climate. This study has shown that transient climate change can significantly affect the area and spatial distribution of potential croplands of the world over the period of 1977–2100. Developed countries account for most of the increase in global potential croplands, while developing countries have little change in the area of potential croplands. The modeling in this study has a spatial resolution of 0.5˚ (longitude) × 0.5˚ (latitude), which can not account for large subgrid variations of land cover and land use, especially in mountainous regions. It will be necessary to conduct similar studies at much finer spatial resolutions (*e.g.*, 5´ longitude by 5´ latitude or even 1 km by 1 km) when global data of climate, vegetation, soil and elevation at finer spatial resolutions are available in the near future.

The incorporation of a global large river network and spatial distribution of human population into the cropland distribution model may improve our estimate of croplands under contemporary climate and provide a basis to assess the effects of water supply (particularly in semi-arid and arid regions) and population dynamics on agriculture in the future. Further work is also needed to model or delineate spatial distributions of various crops on the globe[10] and to estimate yields of crops.

A land use model, which uses potential croplands and social-economic constraints, needs to be developed to define the area and spatial distribution of actual croplands on the globe. The linkage of a land cover and land use change model, a global terrestrial biogeochemistry model (*e.g.*, TEM) and a climate model will allow us to assess the impacts of land cover and land use changes on global carbon and nitrogen cycling as well as the feedbacks of land cover and land use changes to atmosphere and climate over time (*e.g.*, net CO_2 fluxes, albedo and roughness).

Acknowledgments

We thank B.L. Turner II, R.G. Prinn, H.D. Jacoby and R. Eckaus for invaluable discussion and comments on the work and earlier versions of the manuscript. G. Esser provided actual cropland data at country level in 1980 from FAO. This study was supported by the Joint Program on the Science and Policy of Global Change at the Massachusetts Institute of Technology (CE-S-462041), the National Institute of Global Environmental Changes of the Department of Energy (No:901214-HAR), and the Earth Observing Systems Program of NASA (NAGW-2669).

References

1. Grubler, A., 1994, Technology, in: *Changes in Land Use and Land Cover: A Global Perspective*, W.B. Meyer and B.L. Turner II (eds.), Cambridge University Press, New York, p. 287-328.

2. Naylor, R.L., 1996, Energy and resource constraints on intensive agricultural production, *Annual Review of Energy and Environment*, **21**, 99-123.

3. Bullock, P. and H. Le Houerou, 1996, Land degradation and desertification, in: *Climate Change 1995—Impacts, Adaptations and Mitigation of Climate Change: Scientific-Technical Analyses*, Contribution of Working Group II to the Second Assessment Report of the Intergovernmental Panel on Climate Change, R.T. Watson, M.C. Zinyowera, R.H. Moss and D.J. Dokken, (eds.), Cambridge University Press, p. 171-189.

4. World Resource Institute, 1992, *World Resources 1992-1993*, Oxford University Press, Oxford, UK, 385 p.

5. Bradbury, I., R. Kirkby G. and Shen, 1996, Development and Environment: the case of rural industrialization and small-town growth in China, *Ambio*, **25**, 204-209.

6. Douglas, I., 1994, Human settlements, in: *Changes in Land Use and Land Cover: A Global Perspective*, W.B. Meyer and B.L. Turner II (eds.), Cambridge University Press, New York, p. 149-169.

7. FAO, 1978, *Report on the Agro-Ecological Zone project, Vol. 3, Methodology and Results for South and Central America*, World Soil Resources Report, **48**/3, FAO, Rome.

8. Brinkman, R., 1987, Agro-ecological characterization, classification and mapping: Different approaches by the International Agricultural Centers, in: *Agricultural Environments. Characterization, Classification and Mapping*, A.H. Bunting (ed.), C.A.B. International, Wallingford, UK, p. 31-42.

9. FAO/IIASA, 1993, Agro-ecological assessments for national planning: The examples of Kenya, *FAO Soils Bulletin*, **67**, FAO, Rome.

10. Leemans, R. and A.M. Soloman, 1993, Modeling the potential change in yield and distribution of

the Earth's crops under a warmed climate, *Climate Research*, **3**, 79-96.

11. Cramer, W.P. and A.M. Soloman, 1993, Climatic classification and future global redistribution of agricultural land, *Climate Research*, **3**, 97-110.

12. Prinn, R., H. Jacoby, A. Sokolov, C. Wang, X. Xiao, Z. Yang, R. Eckaus, P. Stone, D. Ellerman, J. Melillo, J. Fitzmaurice, D. Kicklighter, Y. Liu and G. Holian, 1996, *Integrated global system model for climate policy analysis: I. Model framework and sensitivity studies*, Joint Program on the Science and Policy of Global Change Report No. **7**, MIT, Cambridge, June, 76 p.

13. Yang, Z., R. Eckaus, D. Ellerman, J. Fitzmaurice and H. Jacoby, 1996, *The MIT Emission Prediction and Policy Analysis (EPPA) model*, Joint Program on the Science and Policy of Global Change Report No. **6**, MIT, Cambridge, Mass., June, 49 p.

14. Wang, C., R. Prinn, A. Sokolov, P. Stone, Y. Liu and X. Xiao, 1995, A coupled atmospheric chemistry and climate model for chemically and radiatively important trace species, WMO-IGAC Conference on the Measurement and Assessment of Atmospheric Composition Change, October, Beijing, WMO GAW No. **107**, 182-184.

15. Yao, M.S. and P.H. Stone, 1987, Development of a two-dimensional zonally averaged statistical-dynamical model. Part I: The parameterization of moist convection and its role in the general circulation, *Journal of the Atmospheric Sciences*, **44**(1), 65-82.

16. Stone, P.H. and M.S. Yao, 1987, Development of a two-dimensional zonally averaged statistical-dynamical model. Part II. The role of eddy momentum fluxes in the general circulation and their parameterization. *Journal of the Atmospheric Science*, **44**(24), 3769-3786.

17. Stone, P.H. and M.S. Yao, 1990, Development of a two-dimensional zonally averaged statistical-dynamical model. Part III. The parameterization of the eddy fluxes of heat and moisture, *J. Climate*, **3(7)**, 726-740.

18. Sokolov, A.P. and P.H. Stone, 1995, *Description and validation of the MIT version of the GISS 2-D Model*, JPSPGC Report No. **2**, MIT, Cambridge, June, 46 p.

19. Xiao, X., D. Kicklighter, J. Melillo, A. McGuire, P. Stone and A. Sokolov, 1997, Linking a global terrestrial biogeochemical model and a 2-D climate model: Implications for the global carbon budget, *Tellus*, **49**B, 18-37.

20. Raich, J.W., E.B. Rastetter, J.M. Melillo, D.W. Kicklighter, P.A. Steudler, B.J. Peterson, A.L. Grace, B. Moore III and C.J. Vorosmarty, 1991, Potential net primary productivity in South America: Application of a global model, *Ecological Applications*, **1**, 399-429.

21. Melillo, J.M., A.D. McGuire, D.W. Kicklighter, B. Moore III, C.J. Vorosmarty and A.L. Schloss, 1993, Global climate change and terrestrial net primary production, *Nature*, **363**, 234-240.

22. McGuire, A.D., J.M. Melillo, D.W. Kicklighter, Y. Pan, X. Xiao, J. Helfrich, B. Moore III, C.J. Vorosmarty and A.L. Schloss, 1997, Equilibrium responses of global net primary production and carbon storage to doubled atmospheric carbon dioxide: sensitivity to changes in vegetation nitrogen concentration, *Global Biogeochemical Cycles*, **11**(2), 173-189.

23. Liu, Y., 1996, *Modeling the emission of nitrous oxide (N_2O) and methane (CH_4) from the terrestrial biosphere to the atmosphere*, JPSPGC Report No. **10**, MIT, Cambridge, Mass., August, 219 p. (Ph.D. Dissertation)

24. Olson, J.S., J.A. Watts and L.J. Allison, 1983, *Carbon in live vegetation of major world ecosystems*, ORNL 5862, Oak Ridge National Laboratory, Oak Ridge, Tenn.

25. Leemans, R. and W.P. Cramer, 1991, *The IIASA climate database for land areas on a grid with 0.5˚ resolution*, Research Report RR-91-18, International Institute for Applied Systems Analysis (IIASA), Laxenburg, Austria, 60 p.

26. Vorosmarty, C.J., B. Moore III, A.L. Grace, M.P. Gildea, J.M. Melillo, B.J. Peterson, E.B. Rastetter and P.A. Steudler, 1989, Continental scale models of water balance and fluvial transport: An application to South America, *Global Biogeochemical Cycles*, **3**(3), 241-265.

27. Jensen, M.E. and H.E. Haise, 1963, Estimating evapotranspiration from solar radiation, *Journal of the Irrigation and Drainage Division*, **4**, 15-41.

28. Beniston, M. and D.G. Fox, 1996, Impacts of climate change on mountain regions, in: *Climate Change 1995—Impacts, Adaptations and Mitigation of Climate Change: Scientific-Technical Analyses*, Contribution of Working Group II to the Second Assessment Report of the Intergovernmental Panel on Climate Change, R.T. Watson, M.C. Zinyowera, R.H. Moss and D.J. Dokken (eds.), Cambridge University Press, p. 191-213.

29. NCAR/NAVY, 1984, *Global 10-minute elevation data*, Digital tape available through National Oceanic and Atmospheric Administration, National Geophysical Data Center, Boulder, Col.

30. Sloss, P.W., 1996, Enhancing NOAA's image: Imagery in print, on walls and on the World Wide Web, *Earth System Monitor*, **7**(1), 1-2, September.

31. FAO-UNESCO, 1971, *Soil map of the world, 1:5,000,000*, UNESCO, Paris, France. Digitization (0.5˚ resolution) by Complex Systems Research Center, University of New Hampshire, Durham, and modifications by Marine Biological Laboratory, Woods Hole of the IPCC IS92 Emission Scenarios, Intergovernmental Panel on Climate Change, Cambridge, UK.

32. IPCC, 1994, *Climate Change 1994: Radiative Forcing of Climate Change and an Evaluation of the IPCC IS92 Emission Scenarios*, Intergovernmental Panel on Climate Change, Cambridge University Press, UK, p. 233-304.

33. Matthews, E., 1983, Global vegetation and land use: New high resolution databases for climate studies, *Journal of Climatology and Applied Meteorololgy*, **22**, 474-487.

34. FAO, 1986, *1985 FAO Production Yearbook, Vol. 39*, Food and Agricultural Organization of the United Nations, Rome.

35. FAO, 1980, *Production Yearbooks, Vol. 33*, FAO Statistics Series No. 28, Food and Agricultural Organization of the United Nations, Rome.

36. Skole, D.L. and C.J. Tucker, 1993, Tropical deforestation and habitat fragmentation in the Amazon: Satellite data from 1978 to 1988, *Science*, **260**, 1905-1910.

37. Fearnside, P.M., 1993, Deforestation in Brazilian Amazonia: The effect of population and land tenure, *Ambio*, **22**, 537-545.

38. Kummer, D. and B. Turner, 1994, The human causes of deforestation in southeast Asia, *Bioscience*, **44**, 323-328.

39. Skole, D.L., W.H. Chomentowski, W.A. Salas and A.D. Nobre, 1994, Physical and human dimensions of deforestation in Amazonia, *Bioscience*, **44**, 314-322.

40. Reilly, J., 1996, Agriculture in a changing climate: Impacts and adaptation, in: *Climate Change 1995—Impacts, Adaptations and Mitigation of Climate Change: Scientific-Technical Analyses*, Contribution of Working Group II to the Second Assessment Report of the Intergovernmental Panel on Climate Change, R.T. Watson, et al. (eds.), Cambridge University Press, p. 427-467.

41. Wittwer, S.H., 1995, *Food, Climate and Carbon Dioxide: The Global Environment and World Food Production,* Lewis Publishers, New York, 236 p.

42. Rosenzweig, C. and M.L. Parry, 1994, Potential impact of climate change on world food supply, *Nature*, **367**, 133-138.

43. Mitchell, J.F.B., S. Manabe, T. Tokioka and V. Meleshko, 1990, Equilibrium climate change and its implications for the future, in: *Climate Change: The IPCC Scientific Assessment,* J.T. Houghton, G.J. Jenkins and J.J. Ephraums (eds.), Cambridge University Press, New York, p. 131-164.

44. Kattenberg, A., F. Giorgi, H. Grassl, G.A. Meehl, J.F.B. Mitchell, R.J. Stouffer, T. Tokioka, A.J. Weaver and T.M.L. Wigley, 1996, Climate models—Projections of future climate, in: *Climate Change 1995: The Science of Climate Change*, J.T. Houghton, L.G. Meira Filho, B.A. Callander, N. Harris, A. Kattenberg and K. Maskell (eds.), Intergovernmental Panel on Climate Change, Cambridge University Press, p. 284-357.

45. Esser, G., 1987, Sensitivity of global carbon pools and fluxes to human and potential climatic impacts, *Tellus*, **39**B, 245-260.

46. Houghton, R., 1996, Terrestrial sources and sinks of carbon inferred from terrestrial data, *Tellus*, **48**B, 420-432.

47. Tobler, W., U. Deichmann, J. Gottsegen and K. Maloy, 1995, *The Global Demography Project*, National Center for Geographical Information and Analysis, Technical Report TR-96-6, Department of Geography, University of California, Santa Barbara, CA 93106.

48. Bulatao, R.A., E. Bos, P.W.S. Stephens and M.T. Vu, 1990, *World Bank Population Projections, 1989–1990 Edition,* John Hopkins University Press, Baltimore, Maryland.